

Electronic Supplementary Information

Direct grafting-from of PEDOT from a photoreactive Zr-based MOF – A novel route to electrically conductive composite materials

Alexander Mohmeyer,^{a,b} Andreas Schaate,^a Bastian Hoppe,^a Hendrik A. Schulze,^a Thea Heinemeyer^a and Peter Behrens^{*a,b}

Abstract: The postsynthetic potential of the two-dimensional metal-organic framework Zr-*bzpd*c-MOF which is based on the photoreactive linker benzophenone-4,4'-dicarboxylic acid (H_2bzpd c) is used here to selectively functionalize the MOF surface. We report the direct radical-induced oxidative grafting-from polymerization of the precursor EDOT on Zr-*bzpd*c-MOF, leading to an electrically conductive composite material and opening the road to a variety of applications.

Contents

1	Materials and Instrumentation	3
1.1	Materials	3
1.2	Instrumentation	3
2	Experimental section	4
2.1	Synthesis of Zr- <i>bzpd</i> c-MOF	4
2.2	Postsynthetic modification with 3,4-polyethoxythiophene (EDOT) and ethanol	4
2.3	Preparation for NMR spectroscopy	4
2.4	Conductivity measurements	5
3	Additional results	6
3.1	SEM images of Zr- <i>bzpd</i> c-MOF crystals	6
3.2	Physisorption results	7
3.3	Energy-dispersive X-ray spectroscopy	8
3.4	Thermogravimetric analysis	13
3.5	Elemental analysis	15
3.6	Solution-state NMR investigations	16
3.7	Theoretical calculations	20
3.8	Conductivity measurements	21
4	Postulated reaction mechanism	23
5	References	25

1 Materials and Instrumentation

1.1 Materials

Zirconium(IV)-oxychloride octahydrate, formic acid, *N,N*-dimethylformamide (DMF) and 3,4-ethylenedioxythiophene were purchased from Sigma Aldrich. Ethanol and acetone were purchased from VWR and benzophenone-4,4'-dicarboxylic acid from abcr Chemicals. All chemicals were used without further purification.

1.2 Instrumentation

X-ray powder diffraction measurements were performed at room temperature using a STOE STADI-P transmission diffractometers equipped with curved Ge(111) monochromators with $\text{CuK}_{\alpha 1}$ radiation ($\lambda = 1.540594 \text{ \AA}$) and a linear position-sensitive detector. The samples were fixed between X-ray amorphous foils.

Scanning electron microscopy and electron-dispersive X-ray spectroscopy were carried out on a JEOL JSM-6700F (2 keV). Solution-state ^1H and ^{13}C NMR spectra were measured on a BRUKER instrument at 400 MHz and were analysed with ACD NMR Processor 12. Physisorption isotherms were measured on an Autosorb 3 instrument from Quantachrome Instruments and were evaluated with the software ASiQwin 2.0 by Quantachrome Instruments. BET areas of the microporous samples were determined with the micropore BET assistant of the accompanying software. TGA data were obtained on a NETZSCH STA 409PC/PG instrument with a heating rate of $10 \text{ K}\cdot\text{min}^{-1}$ with a gas flow of 80% argon and 20% oxygen. Elemental analysis for carbon and sulfur (C-S analysis) was performed with an ELTRA C/S Analyzer and the UNI Software from ELTRA GmbH was used for evaluation. UV irradiation experiments were performed with a high power LED UV Spot from Laser 2000 with a wavelength of 365 nm. Van der Pauw experiments of the electrical conductivity were performed in a glovebox under Ar atmosphere. Conductivity measurements were performed using a self-made 4-point-probe setup with a Keithley 2100 multimeter (Beaverton, USA).

2 Experimental section

2.1 Synthesis of Zr-*bzpd*c-MOF

Solvothermal synthesis of Zr-*bzpd*c-MOF was carried out in Teflon-sealed screw cap glass vessels. Favorable conditions for the synthesis of a product without amorphous impurities are as follows: 3.22 g (10 mmol) $\text{ZrOCl}_2 \cdot 8 \text{H}_2\text{O}$ were dissolved in 200 mL DMF. After adding 56.59 mL formic acid (1.5 mol, 150 molar equivalents (eq) based on the amount of Zr^{4+}) and 8.11 g (30 mmol, 3 eq) H_2bzpd c, the clear solution was transferred in a 500 mL Teflon-sealed glass vessel and was kept at 120 °C for 2 weeks in a circulating air oven. After the reaction, the solution was cooled down to room temperature and the resulting solid was obtained by decanting, washed once with 100 mL of DMF and two times with 50 mL methanol and afterwards dried under reduced pressure. For further investigations the sample was activated via Soxhlet-extraction with acetone for 24 hours. The white powder was kept under reduced pressure until further usage. The resulting Zr-*bzpd*c-MOF crystals have a rhombic shape and a size of about 100 μm (Figure S1). The yield of the synthesis is about 50%.

2.2 Postsynthetic modification with 3,4-polyethoxythiophene (EDOT) and ethanol

For the postsynthetic modification (PSM) with EDOT, 100 mg Zr-*bzpd*c-MOF was dispersed in 2 mL neat EDOT and purged with Ar for 1 hour. Afterwards the dispersion was irradiated under Ar purging for a specific time (between 1 h – 72 h). After isolation of the product, it was washed two times with acetone and then Soxhlet-extracted with acetone for 48 hours. The samples were dried under reduced pressure overnight.

For comparison, a sample in which all the keto groups had reacted was prepared using the PSM with ethanol. The same procedure with 72 hours irradiation under argon purging was applied to Zr-*bzpd*c-MOF in ethanol. A ^{13}C NMR spectrum verified the complete reaction of the keto groups by the absence of a keto carbon signal at about 195 ppm (Figure S9).

2.3 Preparation for NMR spectroscopy

For solution-state NMR experiments, 50 mg of the MOF were dispersed in $[\text{D}_6]\text{DMSO}$. Under vigorous stirring 20 μL aqueous HF (40%) were added and stirred for 18 hours. After complete dissolution of the Zr-*bzpd*c-MOF, an excess of CaCl_2 was added to the clear solution. The supernatant was used for ^1H and ^{13}C BB NMR investigations.

2.4 Conductivity measurements

The Soxhlet-extracted and dried samples (activated in vacuum for at least 24 hours) were pressed into pellets (diameter of 8 mm, thickness between 0.7 – 0.9 mm) by using a hydraulic press for 1 minute at a weight of one ton (≈ 2000 bar). Van der Pauw measurements were performed in a glove box under inert atmosphere in the dark ($O_2 < 0.5$ ppm, $H_2O < 0.5$ ppm). Conductivity measurements were performed using a self-made 4-point-probe setup with a Keithley 2100 multimeter (Beaverton, USA). The van der Pauw method excludes the resistances of contacts and wires so that only the resistance of the material is observed.¹

3 Additional results

3.1 SEM images of Zr-*bzpd*c-MOF crystals

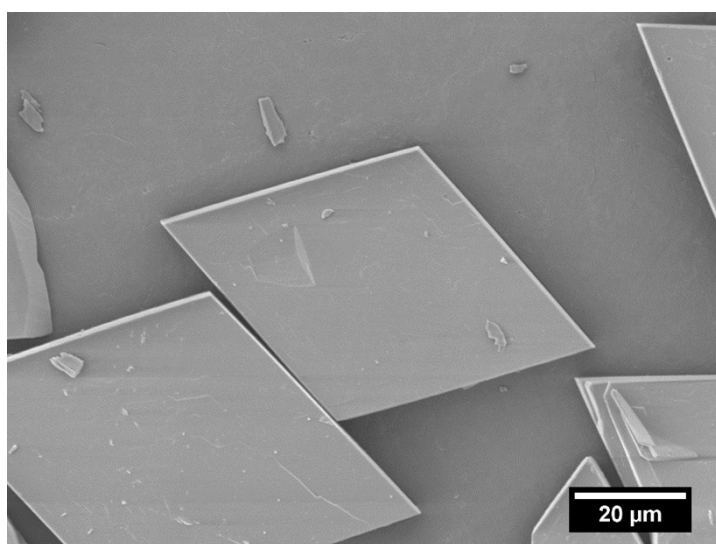
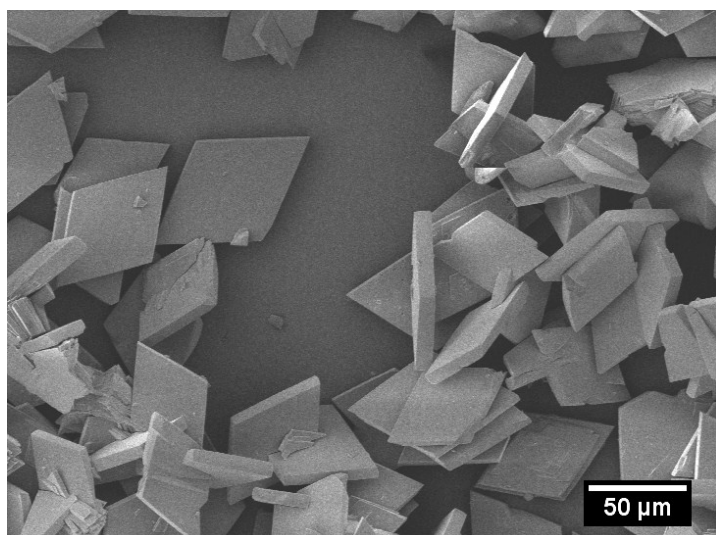
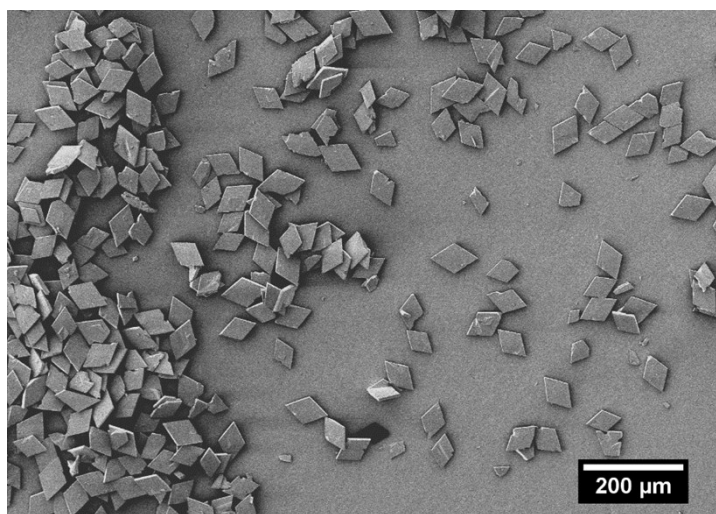


Figure S1. SEM images of single crystals of Zr-*bzpd*c-MOF.

3.2 Physisorption results

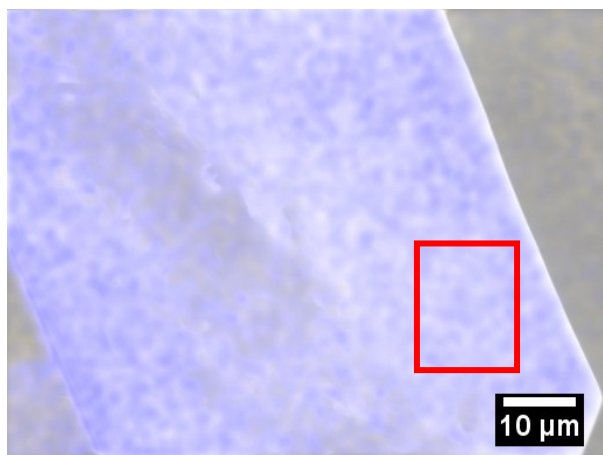
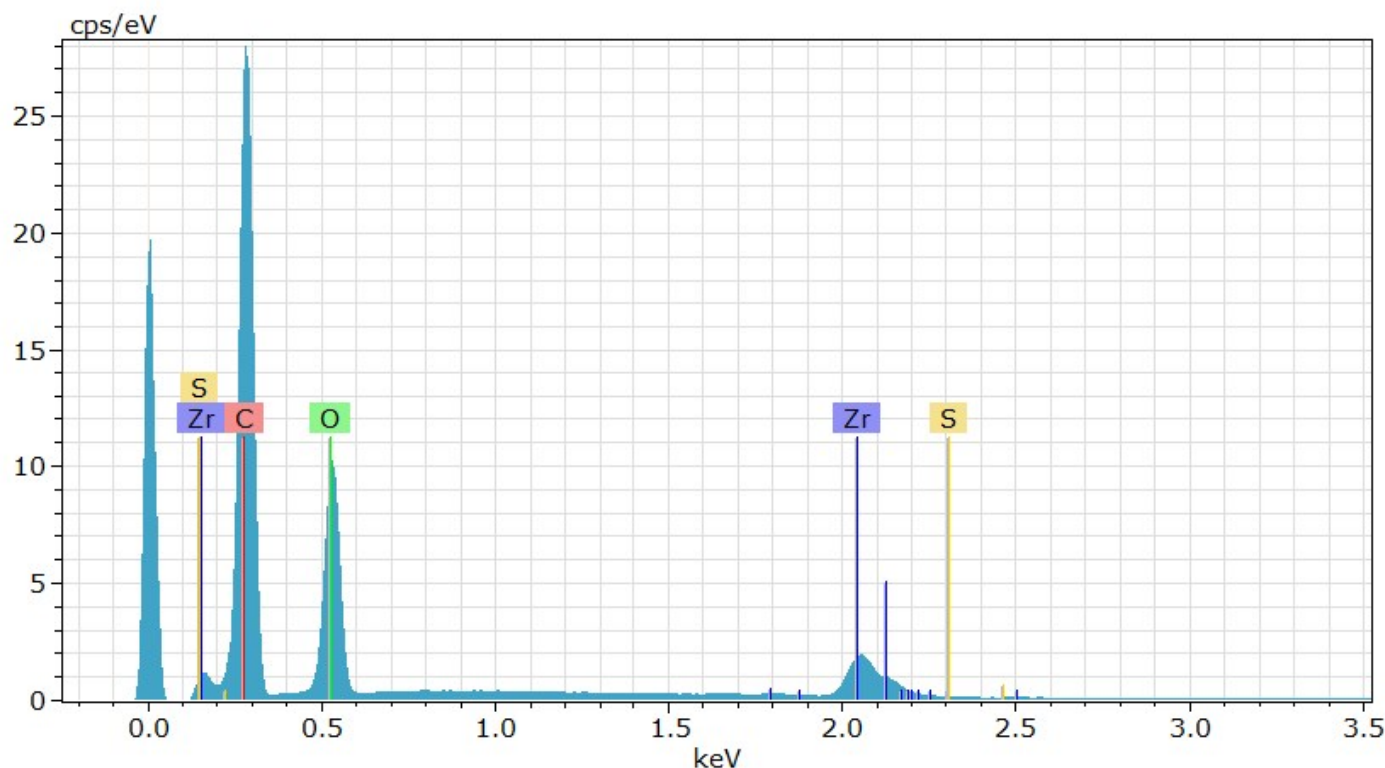
Results of physisorption measurements ($N_2@77K$) are shown in Table S1.

Table S1. Calculated BET areas and total pore volumes for Zr-*bzpd*c-MOF and postsynthetically modified samples with PEDOT.

Sample	BET area / $m^2 \cdot g^{-1}$	Total pore volume / $cm^3 \cdot g^{-1}$
Zr- <i>bzpd</i> c-MOF	670	0.40
UV EDOT 1 h	630	0.37
UV EDOT 6 h	600	0.34
UV EDOT 24 h	570	0.30
UV EDOT 48 h	540	0.26
UV EDOT 72 h	520	0.23

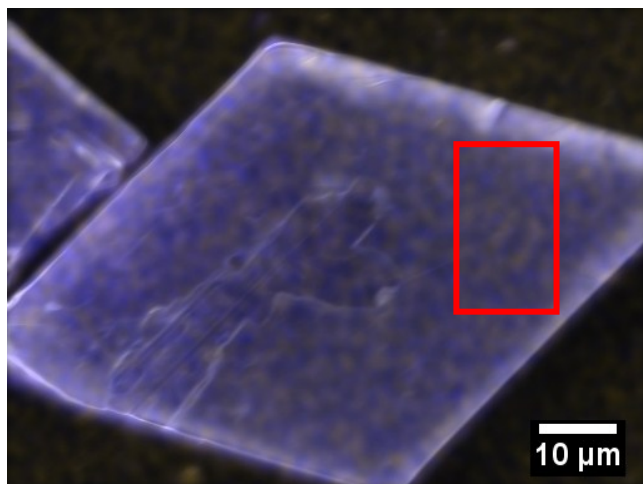
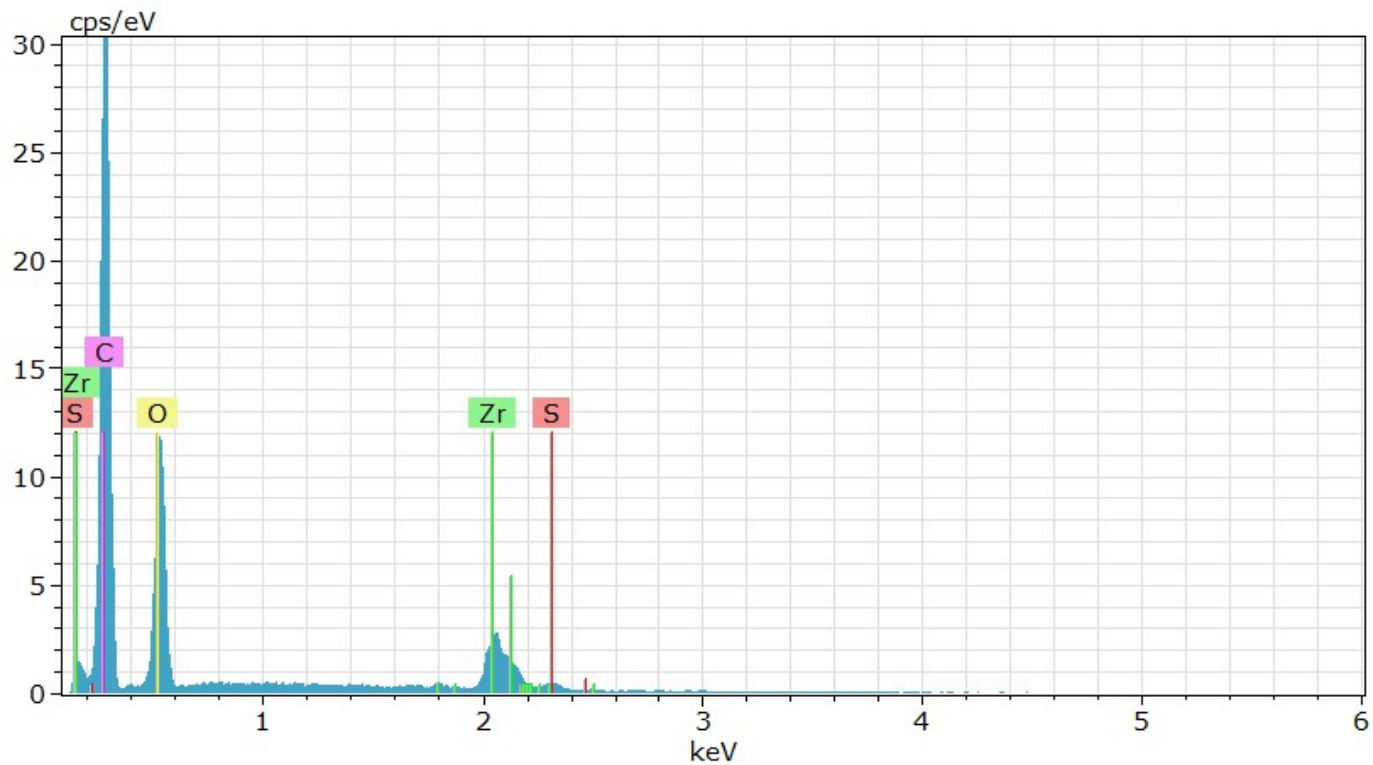
3.3 Energy-dispersive X-ray spectroscopy

Energy-dispersive X-ray spectroscopy is used to display qualitatively the presence of EDOT/PEDOT molecules at the *Zr-bzpd*c-MOF surface through the sulfur signal at about 2.3 keV compared to the zirconium signals at 0.15 keV and 2.05 keV. The results are shown in the following figures for the *Zr-bzpd*c-MOF as-synthesized (Figure S2) and the irradiated samples with 24 h (Figure S3), 48 h (Figure S4) and 72 h (Figure S5) hours of UV light exposure in EDOT, respectively.



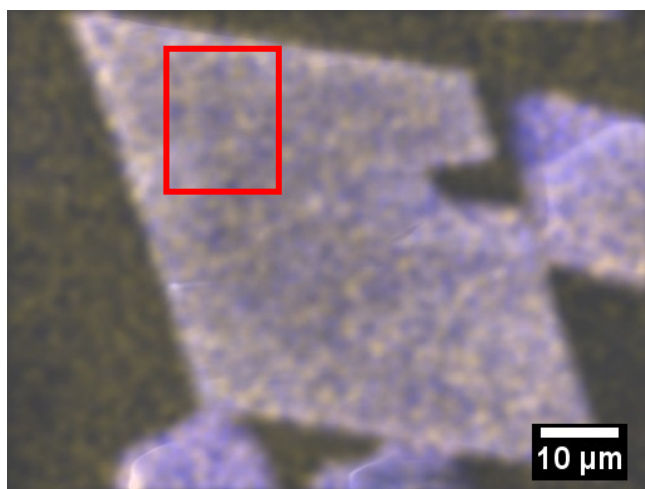
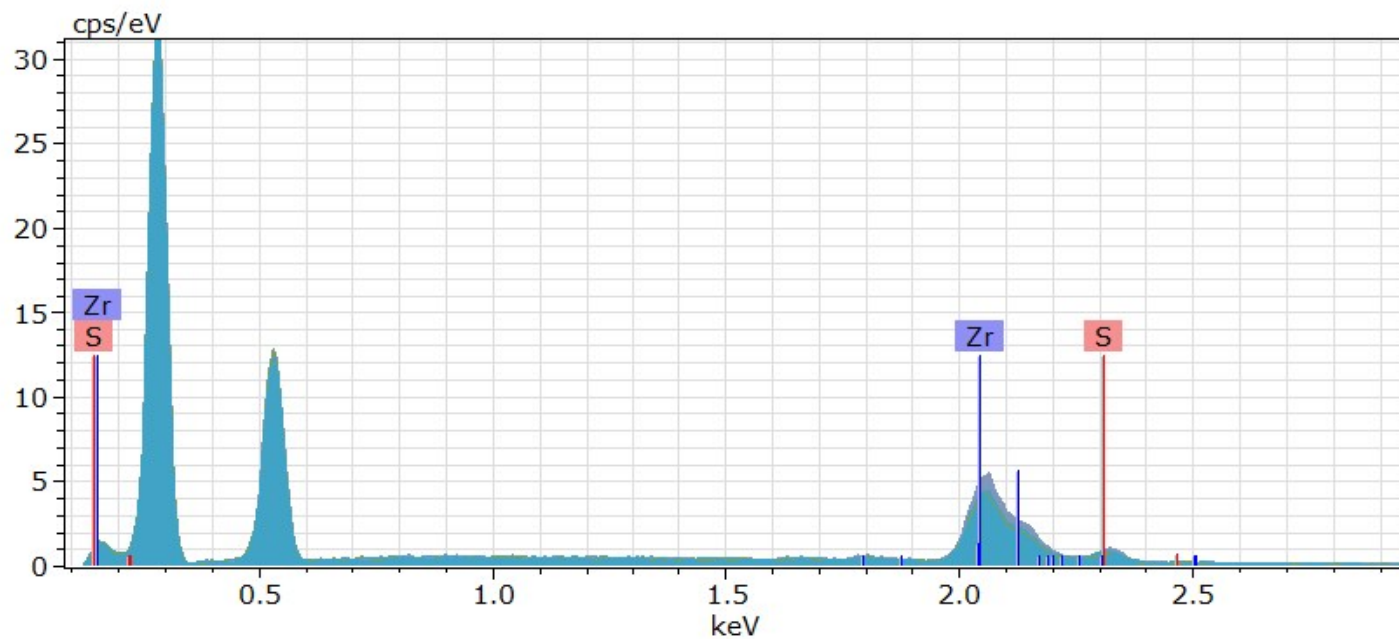
Element	Series	Mass fraction / %	Atom fraction / %
Zirconium	L-series	98.9	97.0
Sulfur	K-series	1.1	3.0

Figure S2. EDXS analysis of *Zr-bzpd*c-MOF as synthesized. Top: EDX spectrum with element assignments. Bottom: Image of measured crystal and the elemental analysis for zirconium and sulfur.



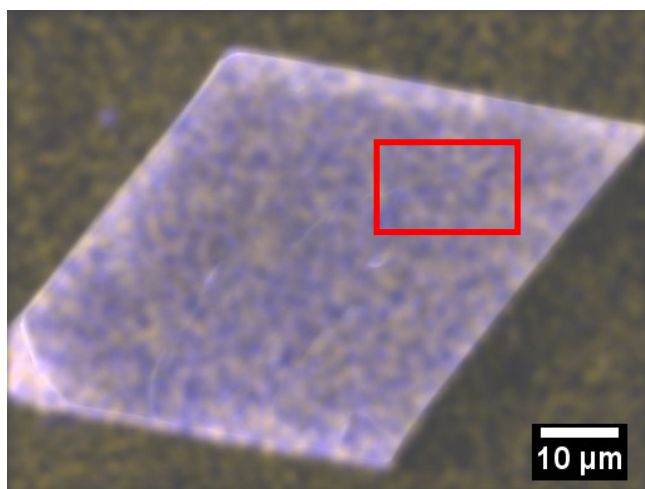
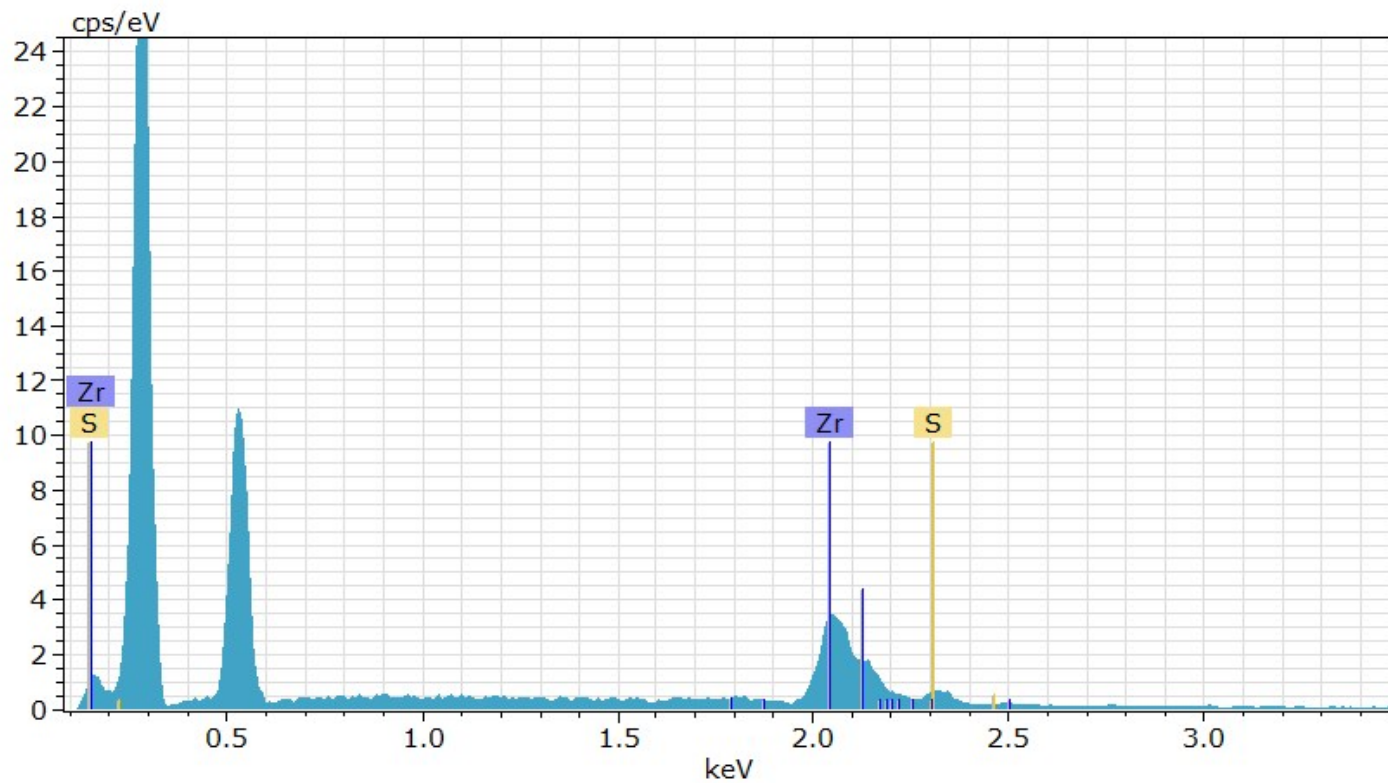
Element	Series	Mass fraction / %	Atom fraction / %
Zirconium	L-series	93.7	83.9
Sulfur	K-series	6.3	16.1

Figure S3. EDXS analysis of irradiated sample for 24 hours. Top: EDX spectrum with element assignments. Bottom: Image of measured crystal and the elemental analysis for zirconium and sulfur.



Element	Series	Mass fraction / %	Atom fraction / %
Zirconium	L-series	91.1	78.2
Sulfur	K-series	8.9	21.8

Figure S4. EDXS analysis of irradiated sample for 48 hours. Top: EDX spectrum with element assignments. Bottom: Image of measured crystal and the elemental analysis for zirconium and sulfur.



Element	Series	Mass fraction / %	Atom fraction / %
Zirconium	L-series	91.4	78.9
Sulfur	K-series	8.6	21.1

Figure S5. EDXS analysis of irradiated sample for 72 hours. Top: EDX spectrum with element assignments. Bottom: Image of measured crystal and the elemental analysis for zirconium and sulfur.

Quantitative data regarding the contents of Zr and S as derived from the EDX results are given in Table S2. Without further calibration, we take these results to qualitatively underline the presence of EDOT/PEDOT in the samples whereby the amount of the sulfur-containing species appears to increase with longer irradiation times.

Table S2. Mass fractions of zirconium and sulfur as calculated from EDXS data.

Sample	Zr / %	Sulfur / %
Zr- <i>bzpd</i> c-MOF	98.9	1.1
UV EDOT 24 h	93.7	6.3
UV EDOT 48 h	91.1	8.9
UV EDOT 72 h	91.4	8.6

3.4 Thermogravimetric analysis

Thermogravimetric analysis curves of Zr-*bzpd*c-MOF and for a sample of Zr-*bzpd*c-MOF postsynthetically modified with EDOT for 72 hours are shown in Figures S6 and S7, respectively.

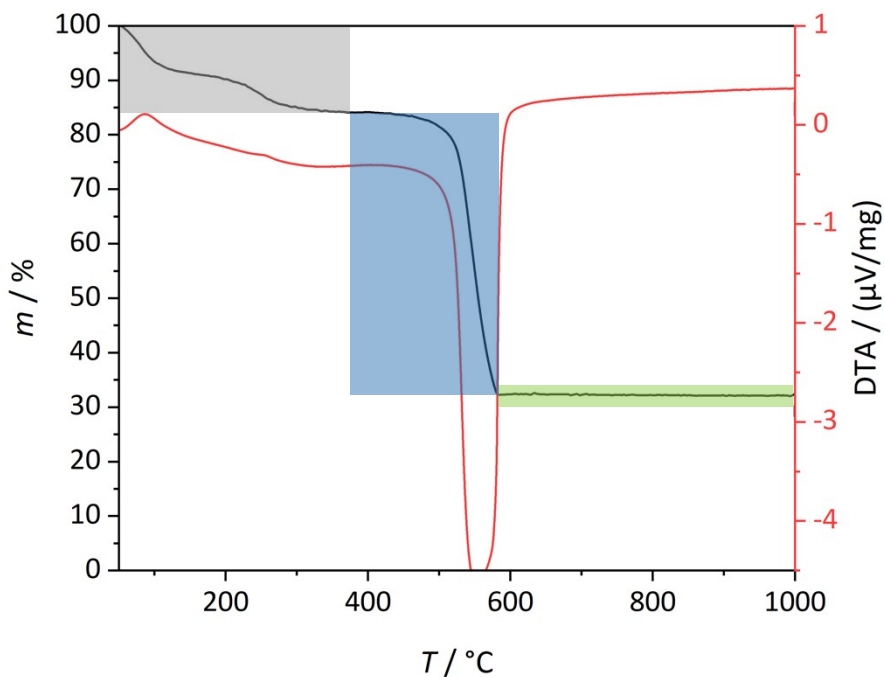


Figure S6. TGA and DTA curves for Zr-*bzpd*c-MOF. (grey: desorption of guest molecules; blue: combined removal of linker molecules and EDOT molecules; green: inorganic residue (ZrO₂))

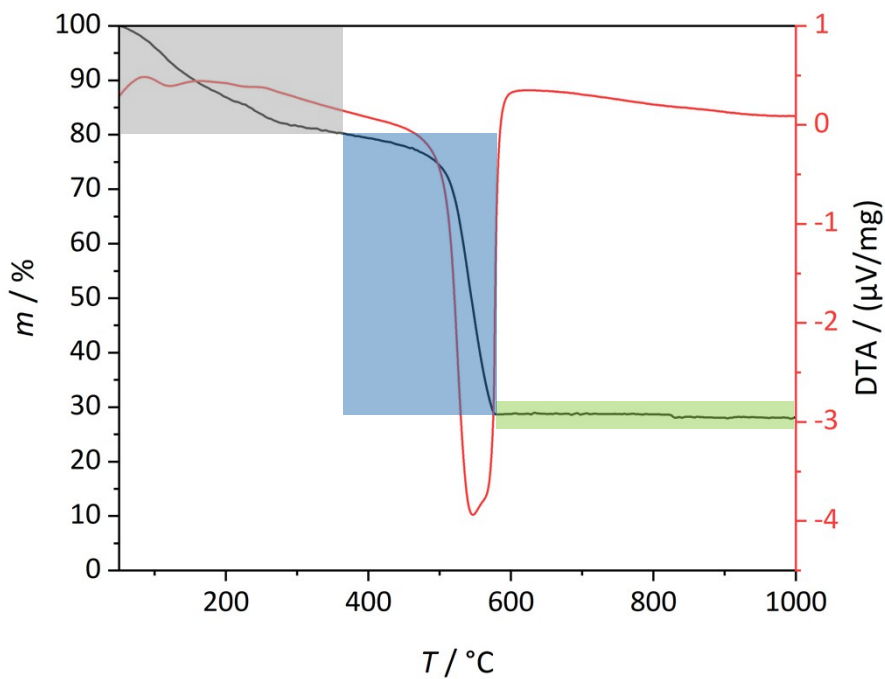


Figure S7. TGA and DTA curves for a sample of Zr-*bzpd*c-MOF postsynthetically modified with EDOT for 72 hours. (grey: desorption of guest molecules; blue: combined removal of linker molecules and EDOT molecules; green: inorganic residue (ZrO₂))

Comparing the amount of the organic contents of Zr-*bzpd*c-MOF to that of postsynthetically modified Zr-*bzpd*c-MOF shows an excess for the latter of about 2.8% of organic molecules which can be ascribed to the presence of EDOT/PEDOT molecules (Table S3). The amount of EDOT/PEDOT is calculated by comparing the “corrected” amounts with the “theoretical” amounts of the organics and the residue originating from the same amount of ZrO₂. Under the assumption that only the keto groups on the outer surface of the MOF crystals react in the photochemical reaction, an approximate average chain length of the PEDOT chains can be calculated (see Section 3.7).

Table S3. Evaluation of the thermogravimetric measurements. Mass fractions derived from thermogravimetric analysis curves of Zr-*bzpd*c-MOF and of Zr-*bzpd*c-MOF postsynthetically modified with EDOT for 72 hours; data are given as “experimental” and “corrected” (after subtraction of the mass loss ascribed to guest molecules).

Zr-<i>bzpd</i>c-MOF	Experimental	Corrected	Theoretical composition for Zr- <i>bzpd</i> c-MOF ²
Guest removal	-17.8%	-	-
Decomposition of organics	-51.3%	-62.4%	-62.8%
Residue (ZrO ₂)	30.9%	37.6%	37.2%

UV EDOT 72 h	Experimental	Corrected	Theoretical composition for Zr- <i>bzpd</i> c-MOF ²
Guest removal	-19.6%	-	-
Decomposition of organics	-51.3%	-63.8%	-62.8%
Residue (ZrO ₂)	29.1%	36.2%	37.2%

3.5 Elemental analysis

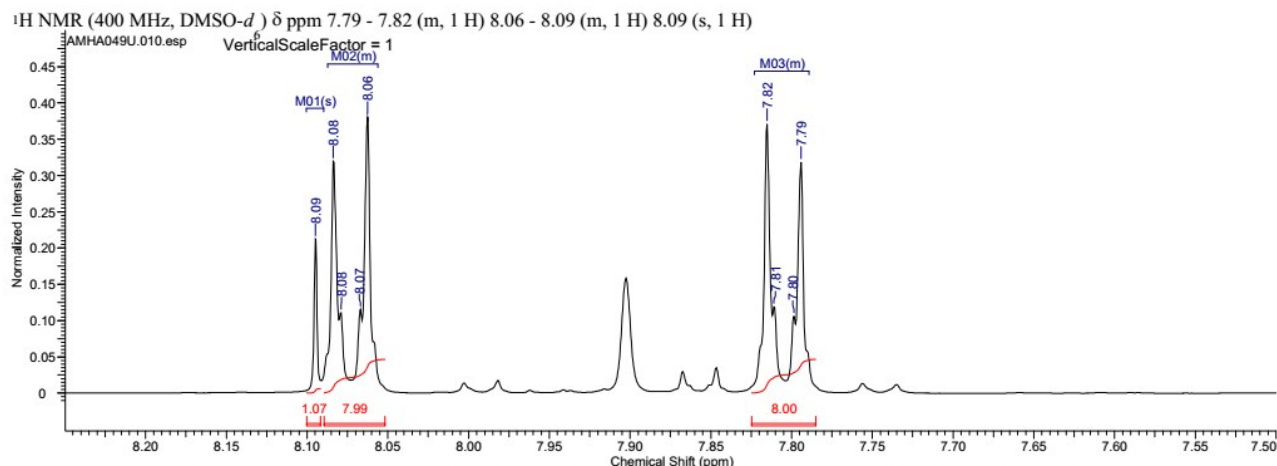
The carbon and sulfur contents were determined via C-S analysis. The results are shown in Table S4. The amount of 0.76% sulfur corresponds to about 3.4% EDOT.

Table S4. Mass fractions of carbon and sulfur as determined via C-S analysis of Zr-*bzpd*c-MOF and of a sample of Zr-*bzpd*c-MOF postsynthetically modified with EDOT for 72 hours.

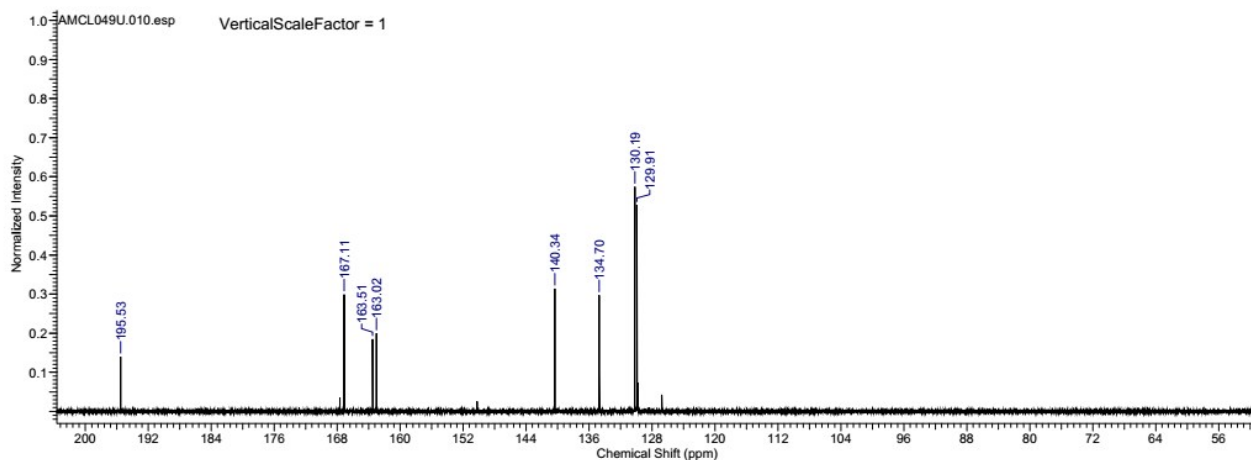
Sample	Carbon / %	Sulfur / %
Zr- <i>bzpd</i> c-MOF	42.94 (15)	0.03 (02)
UV EDOT 72 h	43.80 (12)	0.76 (02)

3.6 Solution-state NMR investigations

NMR spectra of acid-digested Zr-*bzpd*c-MOF show the presence of formic acid in the framework and signals for the benzophenone groups (Figure S8). This is comparable to results already published.² The singlet at about 8.09 ppm represents the formate molecules. The signals for the aromatic protons of benzophenone-4,4'-dicarboxylic acid are contained in the multiplet at 7.79 ppm – 8.08 ppm.



No.	(ppm)	Value	Absolute Value	Non-Negative Value	No.	Shift1 (ppm)	H's	Type	Multiplet1	(ppm)	No.	(ppm)	(Hz)	Height
1	7.850	7.8280000000	3.28000205e+10	8.00000000	1	7.80	1	m	M03	[7.79 .. 7.82]	1	7.79	3119.2	0.3183
2	8.0518	8.08799202394	3.27673180e+10	7.99202394	2	8.07	1	m	M02	[8.06 .. 8.09]	2	7.80	3121.0	0.1060
3	8.0916	8.10147465637	4.40609382e+9	1.07465637	3	8.09	1	s	M01	[8.09 .. 8.10]	3	7.81	3125.9	0.1192
4					4						4	7.82	3127.7	0.3710
5					5						5	8.06	3226.7	0.3807
6					6						6	8.07	3228.4	0.1152
7					7						7	8.08	3233.3	0.1110
8					8						8	8.08	3235.2	0.3194
9					9						9	8.09	3239.6	0.2122



No.	(ppm)	(Hz)	Height
1	129.91	13074.2	0.5275
2	130.19	13102.9	0.5744
3	134.70	13556.2	0.2974
4	140.34	14124.1	0.3139
5	163.02	16406.5	0.2000
6	163.51	16455.4	0.1849
7	167.11	16818.6	0.2987
8	195.53	19678.4	0.1396

Figure S8. ¹H and ¹³C NMR spectra of acid-digested sample of Zr-*bzpd*c-MOF.

For further investigations the keto carbon signal of about 195 ppm is the most important one. The ^{13}C NMR spectrum of the sample postsynthetically modified with ethanol (Figure S9) shows, when compared to the untreated sample, no signal for the keto carbon atom. This indicates a complete reaction of the keto groups with ethanol molecules, leading to the formation of a C-C bond and a hydroxyl group. The ^1H NMR spectrum correspondingly shows a quartet at about 3.45 ppm (methylene group) and a triplet at about 1.05 ppm (methyl group). As no benzophenone groups are present in this sample anymore, the mechanism proposed in the manuscript to explain the conductivity of the pristine Zr-*bzpd*c-MOF is not effective anymore. Correspondingly, no electrical conductivity is measured on this sample.

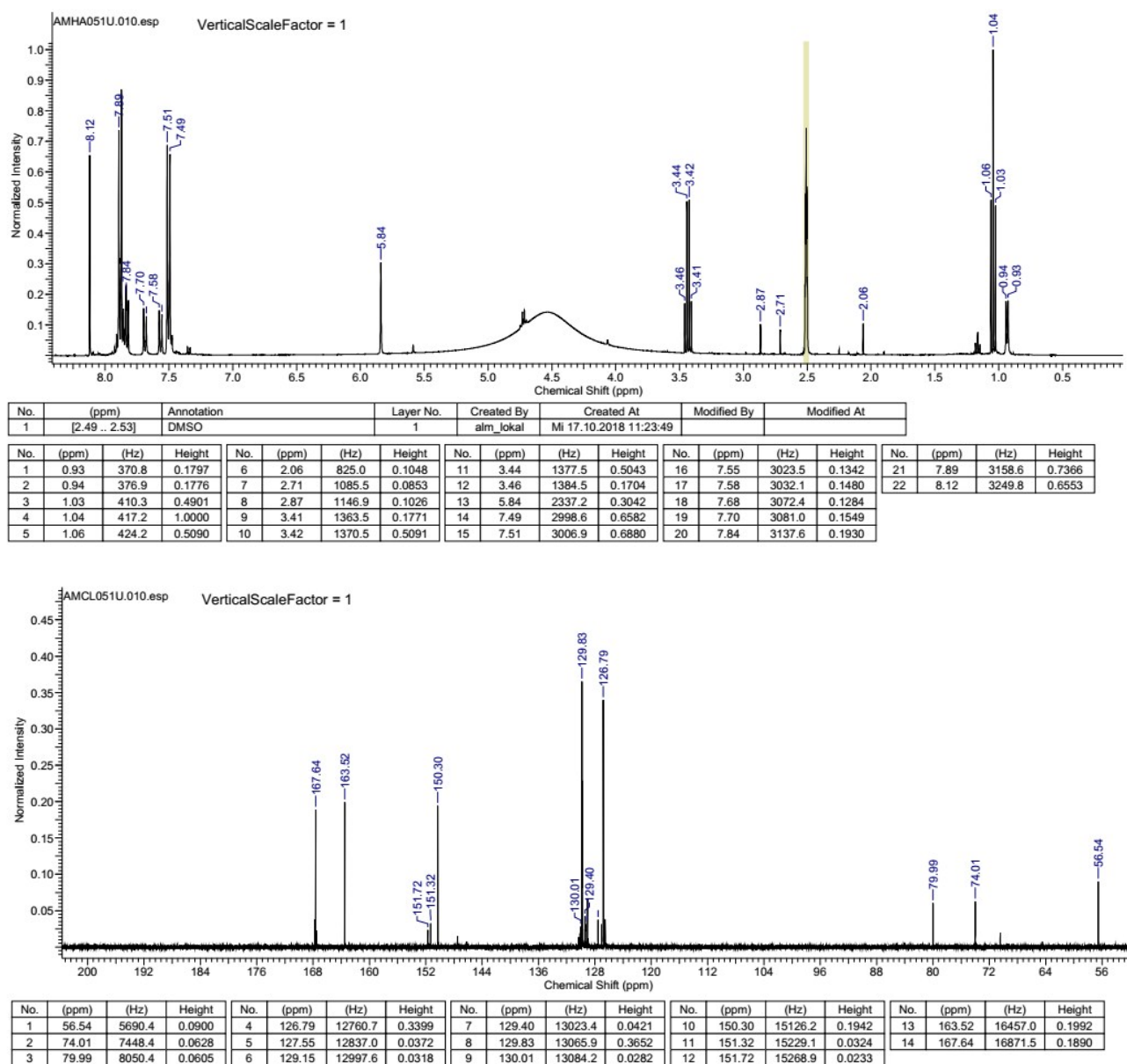
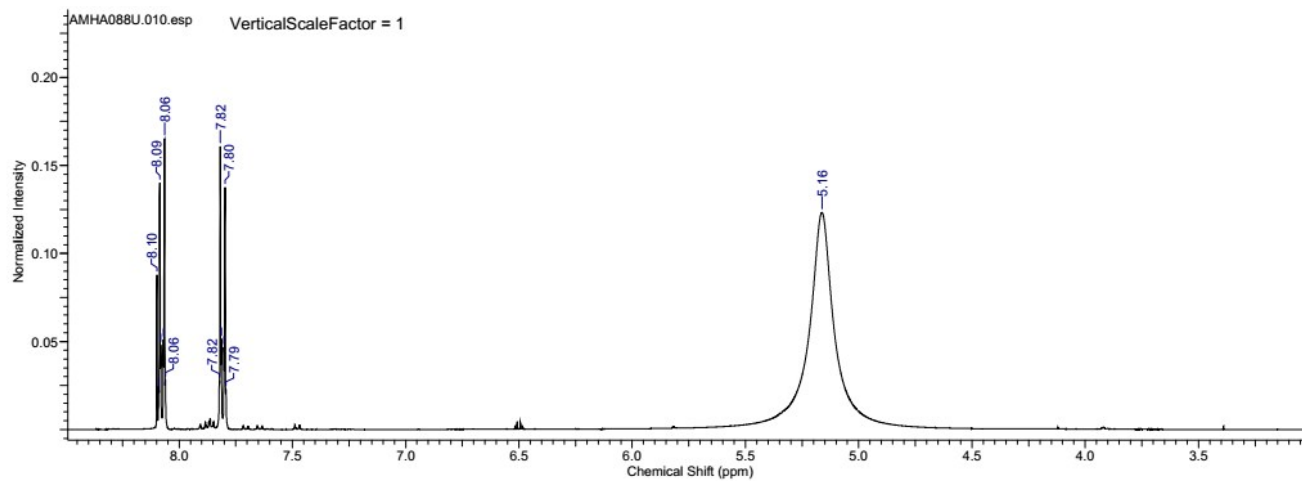
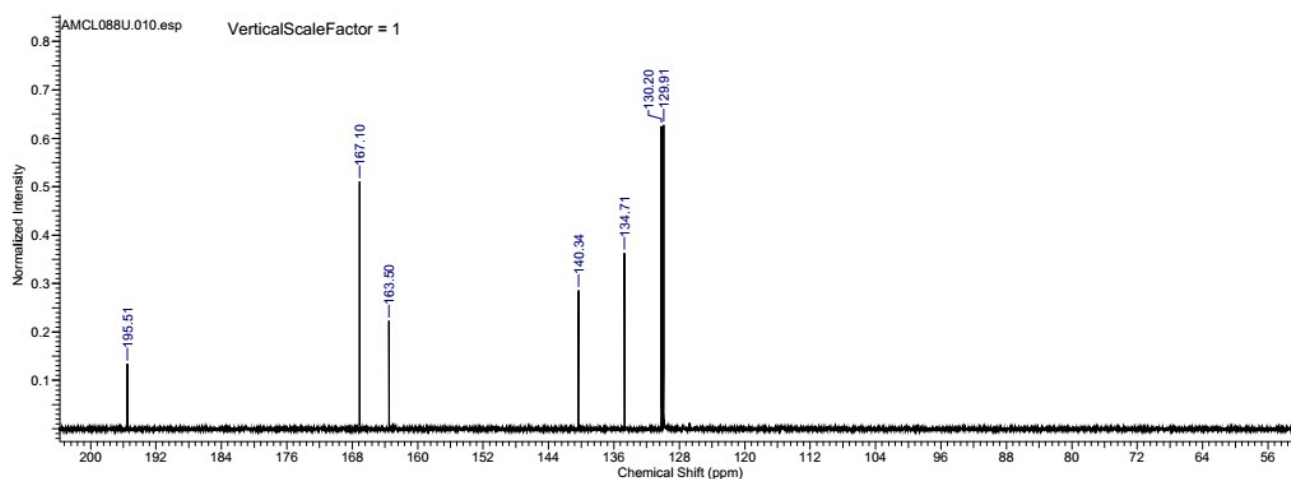


Figure S9. ^1H and ^{13}C NMR spectra of acid-digested Zr-*bzpd*-MOF postsynthetically modified with ethanol.

For a Zr-*bzpd*c-MOF sample postsynthetically modified with EDOT (irradiation for 72 hours) which was dissolved after synthesis, ^1H and ^{13}C NMR spectra are shown in Figure S10. In the ^1H NMR spectrum, signals for thiophene units should appear at about 6.5 ppm. A multiplet with a very low intensity can be observed at this position; however, this signal cannot be quantified. The ^1H NMR spectrum can thus only show the presence of a very small quantity of EDOT units in the dissolved postsynthetically modified sample. We ascribe the fact that no signals are observed for oligo-/polymer chains of PEDOT to the insolubility of PEDOT chains which can then not be detected with solution-state NMR spectroscopy. The presence of the keto carbon signal in the ^{13}C NMR spectrum shows that only a small amount of the keto groups has reacted with EDOT molecules. This is in line with the assumption that only surface-standing keto groups have reacted.



No.	(ppm)	(Hz)	Height	No.	(ppm)	(Hz)	Height	No.	(ppm)	(Hz)	Height	No.	(ppm)	(Hz)	Height
1	5.16	2066.0	0.1233	4	7.80	3122.5	0.0468	7	7.82	3130.6	0.0277	10	8.07	3229.4	0.0510
2	7.79	3119.0	0.0230	5	7.81	3127.2	0.0515	8	8.06	3225.9	0.0282	11	8.08	3234.1	0.0480
3	7.80	3120.4	0.1376	6	7.82	3129.0	0.1608	9	8.06	3227.4	0.1652	12	8.09	3236.0	0.1402



No.	(ppm)	(Hz)	Height
1	129.91	13074.2	0.6278
2	130.20	13103.2	0.6256
3	134.71	13557.0	0.3629
4	140.34	14124.1	0.2862
5	163.50	16454.6	0.2228
6	167.10	16817.4	0.5108
7	195.51	19676.8	0.1344

Figure S10. ^1H and ^{13}C NMR spectra of acid-digested sample of Zr-*bzpdC*-MOF postsynthetically modified with EDOT for 72 hours.

3.7 Theoretical calculations

Based on the fact that

- according to the crystal structure of Zr-*bzpd*c-MOF, keto groups accessible for the PSM are present on the basal planes

and using

- the dimensions of the crystals
- the (theoretical) density of the Zr-*bzpd*c-MOF

as well as

- the contents (mass fractions) of EDOT/PEDOT as derived from TGA and C-S analysis (2.8% and 3.4%, respectively)

we can estimate the lower boundary of the average chain lengths of PEDOT molecules attached to the MOF surface if we make the following additional assumption:

- every surface-standing keto group has initiated the polymerization of a PEDOT chain

This assumption implies that growing polymer chains do not sterically hinder the access of still unreacted surface-standing keto groups and that chain initiation dominates over chain propagation. The distance between surface-standing keto groups is ca. 11 Å; therefore, steric hindrance from grown polymer chains may not be such a strong issue. On the other hand, often chain propagation dominates over chain initiation. With these restrictions in mind, we carried out the following calculations which provide us with an estimate of the lower boundary of the PEDOT chain lengths.

We determined the average size of the basal rhombic planes of the crystals to 4346 μm^2 (average rhombus size: 82 μm x 53 μm , determined with ImageJ on about 30 crystals in Figure S1). The average thickness of the crystals varies more strongly between 5 – 10 μm . For the calculations we use a thickness of 7.5 μm to determine a volume of $1.6298 \cdot 10^{-8}$ cm^3 per crystal. With the theoretical density of $1.16 \text{ g} \cdot \text{cm}^{-3}$ the mass of one crystal is about $1.89 \cdot 10^{-8}$ g. Referring again to the crystal structure model for the Zr-*bzpd*c-MOF, the number of surface-standing keto groups accessible for the photochemical reaction is about $3.0 \cdot 10^9$ per crystal. The

total amount of keto groups is about $2.34 \cdot 10^{13}$ per crystal. A crystal of Zr-*bzpd*c-MOF has about 0.01% keto groups at the outer surface.

1 g of such rhombic shaped Zr-*bzpd*c-MOF crystals thus offers $1.6 \cdot 10^{17}$ keto groups for reaction. The mass of EDOT/PEDOT bound by to this amount of MOF is 28 mg or 34 mg, respectively, depending on the determination method (TG vs. C-S analysis). Distributing this mass of EDOT/PEDOT over $1.6 \cdot 10^{17}$ keto groups, we obtain average chain lengths of about 70 monomer units from the TGA result and of about 90 monomer units from the result of the C-S analysis, respectively. Due to the uncertainties mentioned above, we state with due caution that the grafted-from PEDOT chains have lengths of at least ca. 100 EDOT units.

3.8 Conductivity measurements

Electrical conductivities were measured on pressed pellets. In order to verify that the press procedure did not affect the crystallinity of the samples, PXRD diagrams were measured afterwards (Figure S11).

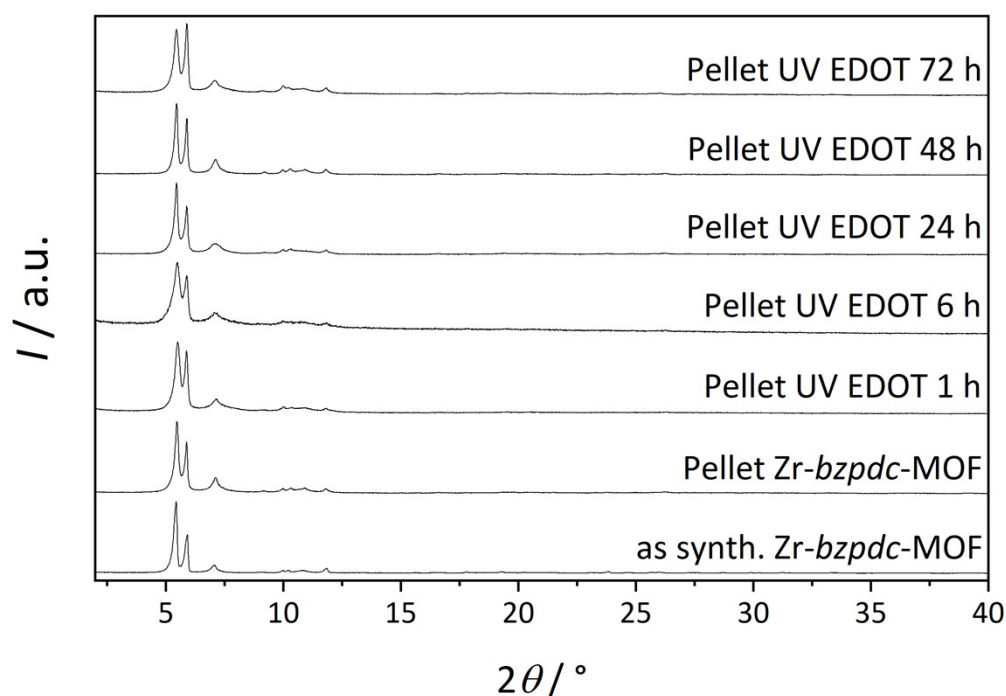


Figure S11. PXRD patterns of pressed pellets after conductivity measurements.

Photographs of pressed pellets with four ohmic contacts (Figure S12) and results from electrical conductivity measurement (Table S5) show the influence of the photochemical polymerization reaction on the color of the samples and on their electrical conductivity.

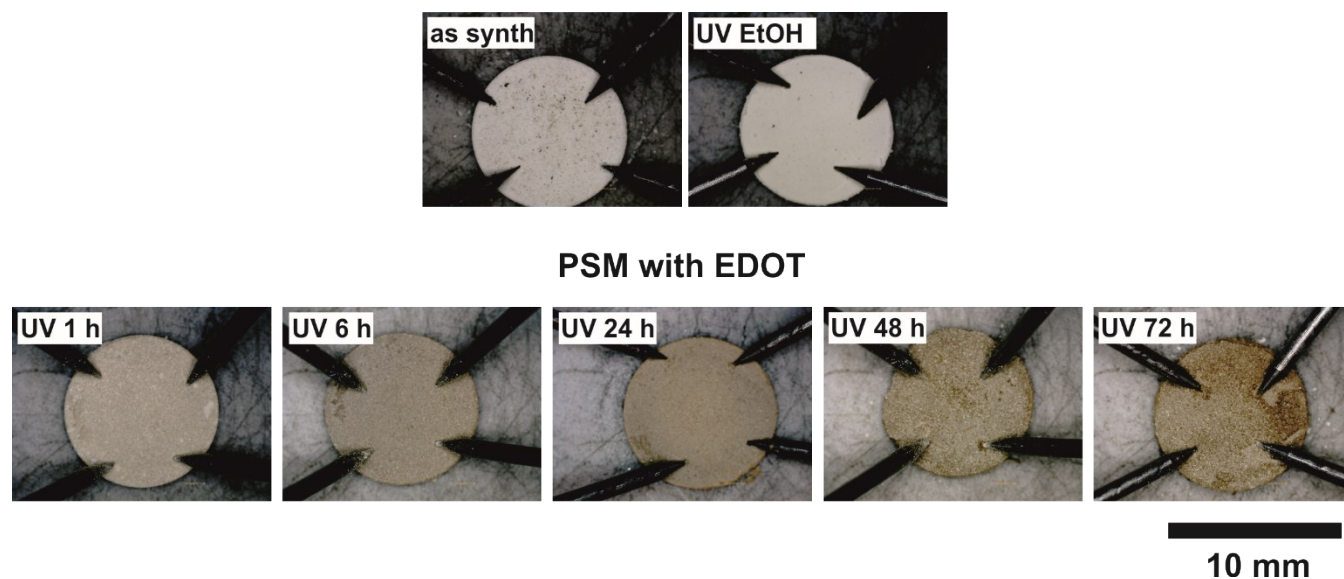


Figure S12. Photographs of the contacted pressed pellets of the samples.

Table S5. Results of electrical conductivity measurements of *Zr-bzpdC*-MOF and postsynthetically modified samples.

Sample	Pellet thickness / nm	Conductivity / S·cm ⁻¹
<i>Zr-bzpdC</i> -MOF	0.78	5.37·10 ⁻⁶
UV EtOH 72 h	0.77	immeasurably low
UV EDOT 1 h	0.80	6.05·10 ⁻⁶
UV EDOT 6 h	0.83	1.07·10 ⁻⁵
UV EDOT 24 h	0.77	8.96·10 ⁻⁴
UV EDOT 48 h	0.74	2.48·10 ⁻³
UV EDOT 72 h	0.75	6.93·10 ⁻³

To visualize the properties of the hybrid materials after different reaction times, we plot the BET area versus the electrical conductivity (Figure S13). The postsynthetic polymerization of EDOT at the MOF surface leads to a slight decrease in porosity. The graph shows impressively that after a reaction time of more than 24 hours the porosity remains about the same (around $500 \text{ m}^2 \text{ g}^{-1}$) whereas the electrical conductivity increases with longer reaction time.

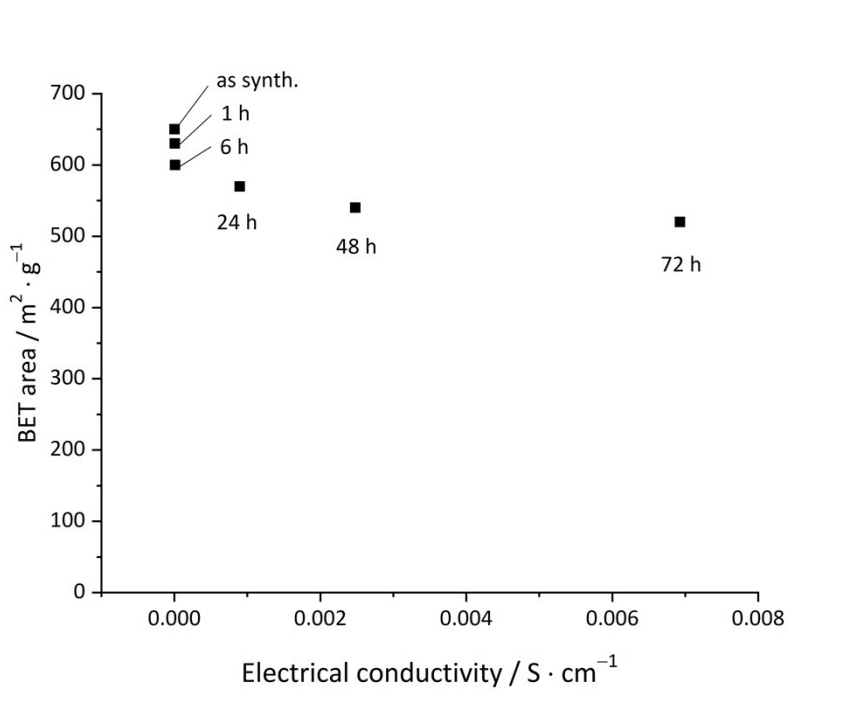


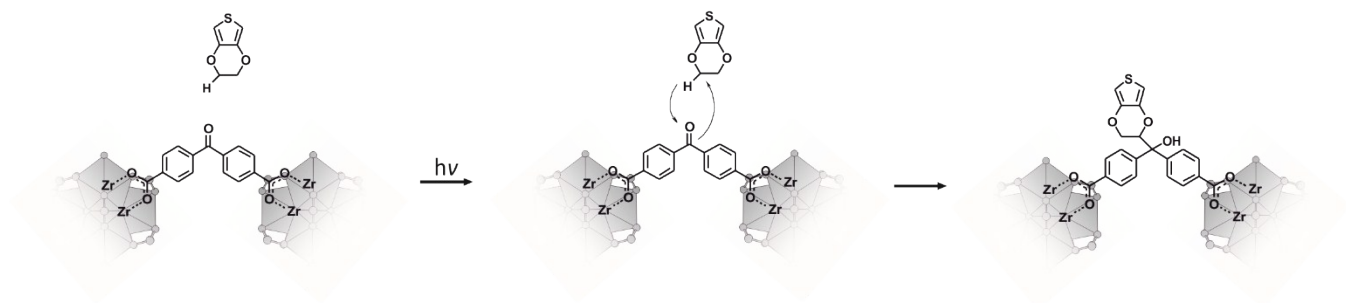
Figure S13. Plot of the BET area versus the electrical conductivity for Zr-*bzpdC*-MOF and postsynthetically modified samples. The reaction times for the postsynthetic reaction are indicated.

4 Postulated reaction mechanism

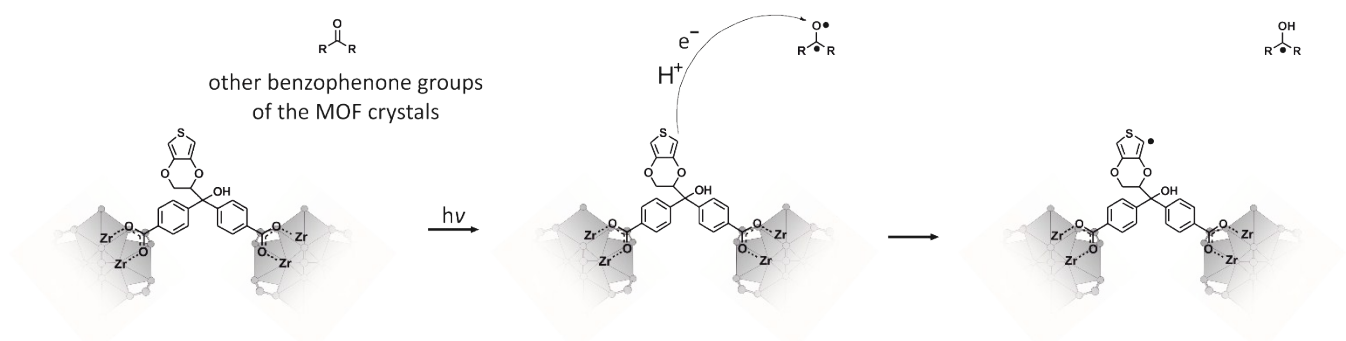
For the polymerization of EDOT at the surface keto groups of the Zr-*bzpdC*-MOF through irradiation, we postulate the reaction mechanism detailed below.

In the first step, we postulate that a photoexcited keto group reacts with a C–H bond of the ethylene group of EDOT, resulting in a covalent bond between the linker molecule and the EDOT unit (of course, this initial reaction could also occur at the thiophene part). This mechanism is well known for the photoreactive benzophenone group (see Scheme 1 of the main paper).³⁻⁵ In general, the following steps could also occur in solution, leading to oligo-/polymers not attached to the MOF surface. However, the following extensive Soxhlet extraction should remove all molecules which are not covalently attached to the MOF. Therefore, we postulate the presence of a covalent bond

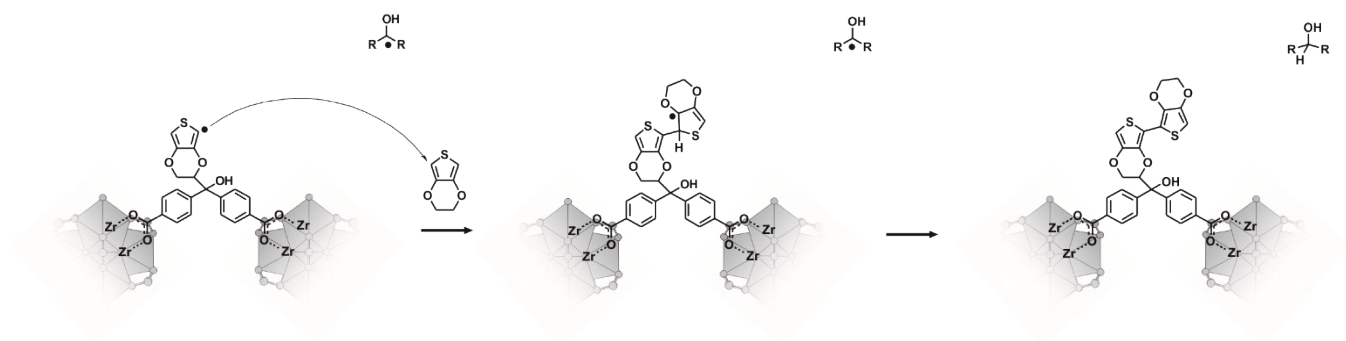
between the MOF crystals and those PEDOT chains which have not been removed by the extraction.



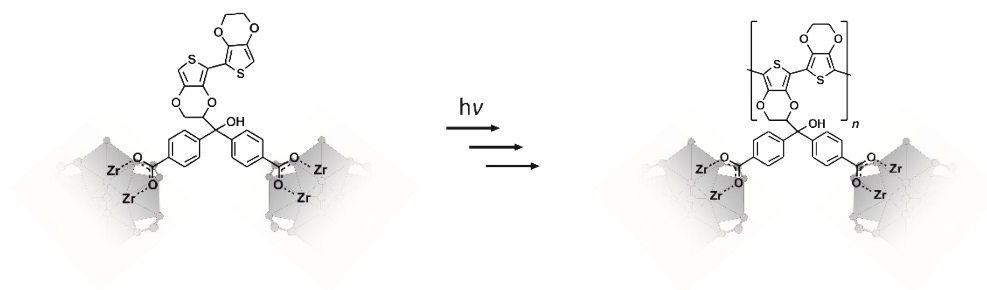
For the second step, we propose the oxidative formation of a radical at the attached EDOT moiety. The only oxidizing agent present in the reaction system is the benzophenone unit of the linker, and in fact, the photo-oxidative potential of irradiated benzophenone⁶⁻⁸ has been described in literature, and the corresponding electron transfer is of course part of the photochemical addition reaction. The shortest distance between two neighbouring keto groups of the MOF crystals is 4.8 Å.



This radical can then attack another EDOT molecule in the third step resulting in a dimer radical. This then loses a hydrogen atom to the ketyl radical, so that on the surface of the MOF crystals the linker molecules actually contain diphenylmethanol groups. The formation of the alcohol group is a consequence of the reduction of the keto group.



The polymerization can then continue under further oxidative radical formation, accompanied by reduction of surface-standing keto groups of the framework.



5 References

- 1 A. A. Ramadan, R. D. Gould and A. Ashour, *Thin Solid Films*, 1994, **239**, 272.
- 2 A. Mohmeyer, A. Schaate, B. Brechtken, J. C. Rode, D. P. Warwas, G. Zahn, R. J. Haug and P. Behrens, *Chem. Eur. J.*, 2018, **24**, 12848.
- 3 D. Karaca Balta, Ö. Karahan, D. Avci and N. Arsu, *Prog. Org. Coat.*, 2015, **78**, 200
- 4 M. A. Winnik and U. Maharaj, *Macromolecules*, 1979, **12**, 902
- 5 O. Prucker, C. A. Naumann, J. Rühle, W. Knoll and C. W. Frank, *J. Am. Chem. Soc.*, 1999, **121**, 8766.
- 6 N. Filipescu and F. L. Minn, *J. Am. Chem. Soc.*, 1968, 90, 1544–1547
- 7 B. Qu, Y. Xu, L. Ding and B. Rånby, *J. Polym. Sci. A Polym. Chem.*, 2000, **38**, 999–1005.
- 8 A. Demeter, K. Horváth, K. Böör, L. Molnár, T. Soós and G. Lendvay, *J. Phys. Chem. A*, 2013, **117**, 10196–10210.